



香港城市大學
City University of Hong Kong

專業 創新 胸懷全球
Professional · Creative
For The World

CityU Scholars

A Transparent Proximity-Coupled-Fed Patch Antenna with Enhanced Bandwidth and Filtering Response

Hu, Hao-Tao; Chen, Bao-Jie; Chan, Chi Hou

Published in:
IEEE Access

Published: 01/01/2021

Document Version:
Final Published version, also known as Publisher's PDF, Publisher's Final version or Version of Record

License:
CC BY

Publication record in CityU Scholars:
[Go to record](#)

Published version (DOI):
[10.1109/ACCESS.2021.3061203](https://doi.org/10.1109/ACCESS.2021.3061203)

Publication details:
Hu, H-T., Chen, B-J., & Chan, C. H. (2021). A Transparent Proximity-Coupled-Fed Patch Antenna with Enhanced Bandwidth and Filtering Response. *IEEE Access*, 9, 32774-32780. [2474].
<https://doi.org/10.1109/ACCESS.2021.3061203>

Citing this paper

Please note that where the full-text provided on CityU Scholars is the Post-print version (also known as Accepted Author Manuscript, Peer-reviewed or Author Final version), it may differ from the Final Published version. When citing, ensure that you check and use the publisher's definitive version for pagination and other details.

General rights

Copyright for the publications made accessible via the CityU Scholars portal is retained by the author(s) and/or other copyright owners and it is a condition of accessing these publications that users recognise and abide by the legal requirements associated with these rights. Users may not further distribute the material or use it for any profit-making activity or commercial gain.

Publisher permission

Permission for previously published items are in accordance with publisher's copyright policies sourced from the SHERPA RoMEO database. Links to full text versions (either Published or Post-print) are only available if corresponding publishers allow open access.

Take down policy

Contact lbscholars@cityu.edu.hk if you believe that this document breaches copyright and provide us with details. We will remove access to the work immediately and investigate your claim.

Received February 9, 2021, accepted February 17, 2021, date of publication February 22, 2021, date of current version March 2, 2021.

Digital Object Identifier 10.1109/ACCESS.2021.3061203

A Transparent Proximity-Coupled-Fed Patch Antenna With Enhanced Bandwidth and Filtering Response

HAO-TAO HU^{1,2}, BAO-JIE CHEN¹, (Member, IEEE), AND CHI HOU CHAN^{1,2}, (Fellow, IEEE)

¹State Key Laboratory of Terahertz and Millimeter Waves, City University of Hong Kong, Hong Kong, SAR

²Department of Electrical Engineering, City University of Hong Kong, Hong Kong, SAR

Corresponding author: Chi Hou Chan (eechic@cityu.edu.hk)

This work was supported by the Grant of the China Science and Technology Exchange Center, the Ministry of Science and Technology, China under Grant 2017/YFE0190400.

ABSTRACT This paper introduces a novel transparent proximity-coupled-fed patch antenna with enhanced impedance bandwidth and good filtering response. The proposed antenna consists of a ground plane, a specific feeding structure and a slotted patch. All the conducting surfaces are realized with metal meshes printed on glass substrates. Optical transparency of the antenna depends on the mesh density. The feed line of a traditional proximity-coupled-fed patch antenna is terminated with a driven stub etched with a half-wavelength U-shaped slot. This modification introduces an additional resonant mode but also a radiating null. By further etching a pair of quarter-wavelength open slots on the radiating patch, another resonant mode accompanied with an extra radiation null is generated. Finally, three resonant modes within the operating band along with two radiation nulls near the two edges of the passband are achieved. The proposed antenna is implemented to demonstrate an impedance bandwidth of 7.6% from 3.41 to 3.68 GHz and a maximum gain of 4.6 dBi.

INDEX TERMS Transparent antenna, filtering antenna, proximity-coupled-fed, bandwidth enhancement, metal mesh structure.

I. INTRODUCTION

In recent years, optical transparent antennas are gaining increasing attention in both the academia and industry due to their see-through characteristic. Since they can be seamlessly attached to automotive windscreens, solar panels, display panels, building windows as well as indoor ceilings and walls, they present great potential for applications in satellite communications, mobile communications and indoor wireless communications.

One common approach to design transparent antenna is the use of the transparent conducting oxides (TCOs) such as indium tin oxide (ITO) [1], [2] and silver-coated polyester (AgHT) films [3], [4]. However, these films always suffer from high sheet resistance subject to their intrinsic characteristic. To further lower the sheet resistance, multilayered films (MLFs) combining TCO and metal are used. They include but not limited to Cu/ITO [5], ITO/Cu/ITO [1], [6]

and IZTO/Ag/IZTO [7], (indium-zinc-tin oxide). Nevertheless, the aforesaid films usually exhibit thin thickness, which makes them basically inappropriate for design of microstrip antennas due to the large skin depth loss [8].

An alternative method is to use metal mesh structures [9]–[13]. It can achieve good balance between the transparency and conductivity by means of controlling the size of the meshes. By selecting appropriate thickness of the metal, skin depth loss can be greatly alleviated. However, these antennas still suffer limited bandwidth or high profile. On the other hand, research on the integration of antenna and filter is also gaining increasing popularity in recent years [14]–[19]. Such integration, coined the term filtering antenna, can make the RF (radio frequency) front end more compact and highly efficient as the filter together with the connection part can be removed.

In this paper, we propose and investigate a novel transparent proximity-coupled-fed antenna with enhanced bandwidth as well as good filtering response. To the authors' best knowledge, it is the first time that a whole-structure-see-through


The associate editor coordinating the review of this manuscript and approving it for publication was Chan Hwang See .

TABLE 1. Dimensions of the filtering antenna element (Unit: mm).

Parameter	P_W	P_L	S_W	S_L	S_D	T_W	T_L	U_{W1}	U_{W2}	U_{L1}
Value	20.46	16.82	0.82	8.07	11.22	5.34	10.94	0.54	0.96	8.39
Parameter	U_{L2}	U_D	M_W	M_L	M_D	F_{W1}	F_{W2}	F_L	G_W	G_L
Value	3.06	1.42	0.86	2.94	3.06	1.76	0.58	9.8	10.56	4.9

filtering antenna without cascading any filtering circuit has been presented. By utilizing well-designed feeding structure and slotted patch, three resonant modes along with two radiation nulls are obtained. Glass substrates and metal mesh structure are employed to realize good light transmittance. The proposed antenna features threefold advantage of enhanced impedance bandwidth, good filtering response and good optical transparency compared to the traditional proximity-coupled-fed patch antenna.

II. ANTENNA STRUCTURE AND WORKING MECHANISM

A. ANTENNA STRUCTURE

Although a few filtering antennas [14]–[19] have been reported in recent years, they either suffer from complicated structure or requirement of drilling and soldering. Note that for PCB (printed-circuit-board) technology, their fabrications may not be a problem. However, for transparent antenna especially designed on glass substrate, one hopes that the antenna structure should be as simple as possible. Besides, drilling and soldering should also be avoided due to the fragile characteristic of the glass as well as for aesthetic consideration. Featuring no requirement of drilling and intact ground plane, the transparent proximity-coupled-fed patch antenna is undoubtedly a good candidate to be attached to indoor ceilings and walls for indoor wireless communications or on windshields of vehicles for vehicle-to-vehicle communications. Our target is to realize a novel transparent proximity-coupled-fed antenna with improved bandwidth and good filtering response.

The geometry of the proposed filtering antenna structure is depicted in Fig. 1, while its dimensions are listed in Table 1. The antenna is realized using two glass substrates with a thickness h of 1.1 mm, dielectric constant ϵ_r of 5.5, and loss-tangent δ of 0.005. Silver mesh with physical parameters of strip gap $s = 120 \mu\text{m}$, strip width $w = 20 \mu\text{m}$, and strip thickness $t = 5.5 \mu\text{m}$ is utilized to implement the metal part of the antenna. This choice is a good tradeoff between optical transparency and antenna efficiency. The sheet resistance can be calculated as 0.02 ohm/square [13]. There are three layers of patterns which are respectively the ground plane on the lower surface of Glass 2, the feeding structure on the upper surface of Glass 2 as well as the radiating patch on the upper surface of Glass 1. The radiating patch is proximity-coupled by the driven stub of the feeding structure. To obtain good filtering characteristic, two techniques have been introduced. First, a U-shaped slot working at half-wavelength resonance is etched on the driven stub, resulting in a radiation null in the lower band. Second, a pair of quarter-wavelength open slots is cut from the radiating patch, generating another

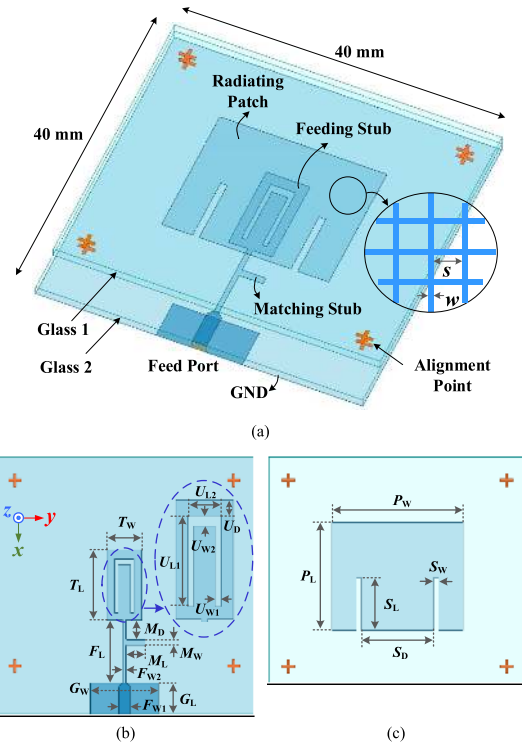


FIGURE 1. Configuration of the proposed transparent filtering antenna. (a) 3D view. (b) Top view of top substrate (Glass 1). (c) Top view of bottom substrate (Glass 2).

radiation null in the upper band. Finally, not only a good filtering response is achieved but also extra resonant modes are introduced, contributing to improvement on the impedance bandwidth.

B. OPERATING PRINCIPLE

To better demonstrate the evolution of the proposed antenna, four referenced designs have been explored as shown in Fig. 2. Design I is a traditional proximity-coupled-fed patch antenna. The end of the feeding line is then modified as a driven stub etched with a half-wavelength U-shaped slot as shown in Design II. On the basis of Design II, a pair of quarter-wavelength open slots is cut from the radiating patch, forming Design III. Finally, a matching stub is added in the feeding line to achieve better impedance matching, leading to Design IV, the proposed antenna.

Performances of the four designs are depicted in Fig. 3. As seen, for the glass substrates we use, the bandwidth of the traditional proximity-coupled patch antenna is limited as only one resonant mode is achieved with slow roll off of the antenna gain, showing little filtering response. After introducing the driven stub along with the U-shaped slot, an extra resonant mode together with a radiation null at the lower band (f_L, f_{Null1}) is brought in. Furthermore, by etching a pair of slots in the radiating patch, another resonant mode and radiation null at the higher band (f_H, f_{Null2}) are introduced. Finally, in Design IV, by adding a matching stub in the feeding line, better impedance matching is obtained.

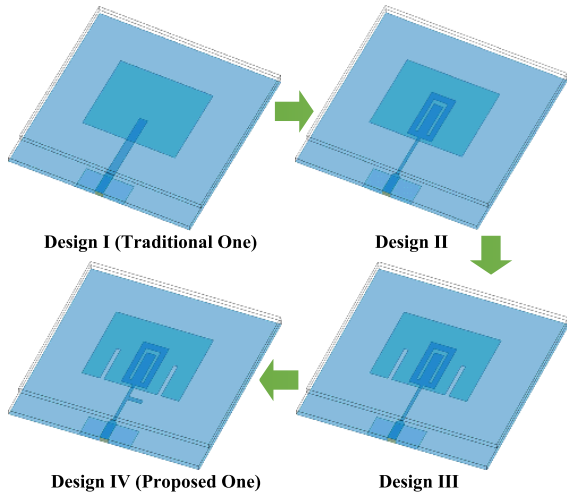


FIGURE 2. Evolution of the proposed transparent filtering antenna.

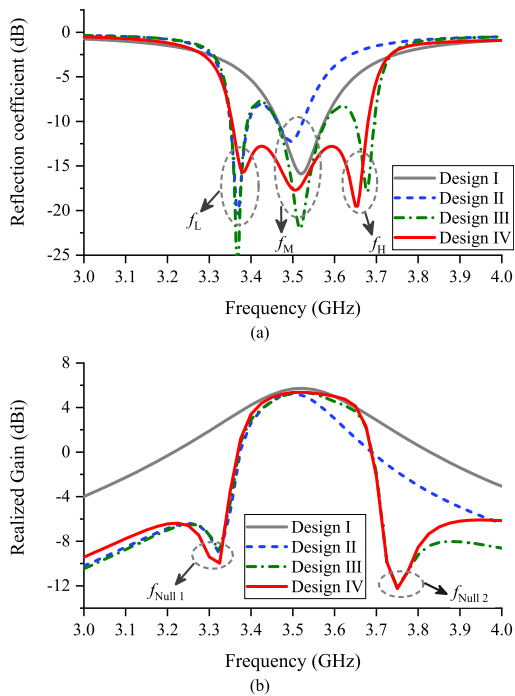


FIGURE 3. Performances of the four referenced antennas. (a) Reflection coefficient. (b) Realized gain.

1) ANALYSIS OF RESONANT MODES AND RADIATION NULLS

To gain more insight into the generation of extra resonant modes and radiation nulls, Designs I, II and III have been investigated from the input impedance's point of view. Their input impedances (Z_{in}) are depicted in Fig. 4. Comparing Design I and Design II, it can be observed that a new peak at the lower band shows up. Consequently, an extra resonant mode shows up at frequency f_L , where the imaginary part of Z_{in} is zero, while the real part roughly equals to 50Ω . At frequency f_{Null1} , Z_{in} approaches to zero, thus generating a radiation null. For Design III, an extra peak appears at the higher band. Similarly, this not only introduces a radiation null at frequency f_{Null2} , where Z_{in} approaches to infinity,

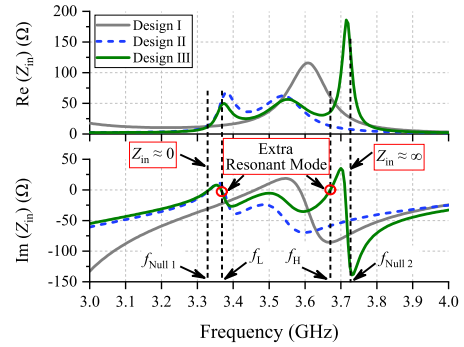


FIGURE 4. Input impedances of Designs I, II and III.

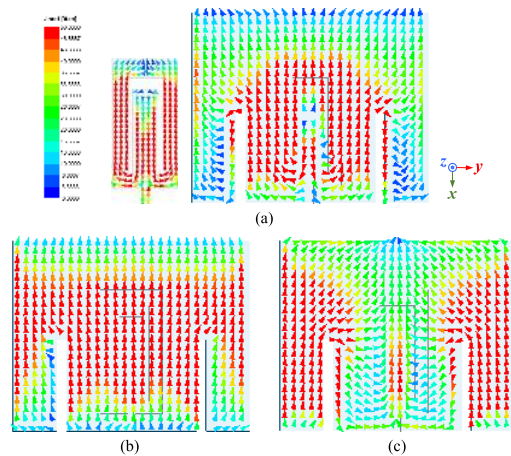


FIGURE 5. Current distributions on feeding stub and radiating patch of Design IV at three resonant frequencies as shown in Fig. 3(a). (a) f_L , 3.38 GHz. (b) f_M , 3.5 GHz. (c) f_H , 3.65 GHz.

but also adds an additional resonant mode at frequency f_H . As seen, the generation principles of the radiation nulls are actually quite different. However, they are in common that large impedance mismatch is caused, leading to little radiation.

Current distributions have also been explored to have intuitive sense of the working mechanism. Fig. 5 depicts the current distribution on the feeding stub and radiating patch of the final design (Design IV) at three resonant frequencies. It can be concluded that these three resonant modes are respectively produced by the driven stub, the fundamental mode and higher-order mode of the patch. Although the length of the driven stub is short, due to the U-shaped slot etched on the stub, its effective length is far longer than the physical length. In other word, it can be regarded as a meandering stub. From Fig. 5(a), we observe that the driven stub works in half wavelength. The fundamental mode of the patch is TM_{10} mode, while the higher-order mode can be regarded as modified TM_{12} mode. Normally, TM_{12} mode cannot well radiate because of the transverse (y-direction) opposite currents. However, in the proposed antenna, these currents can be cut off by the slot as shown in Fig. 5(c). Note that despite a small part of currents are still reversely oriented on the patch, most of the currents travel along the

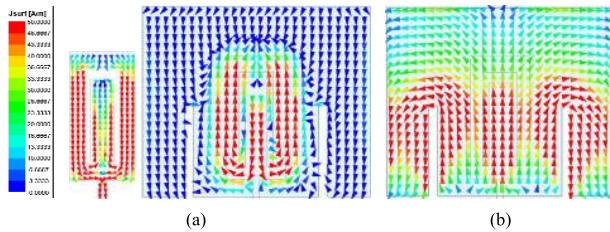


FIGURE 6. Current distributions on feeding stub and radiating patch of Design IV at two radiation null frequencies. (a) $f_{\text{Null}1}$, 3.32 GHz, (b) $f_{\text{Null}2}$, 3.75 GHz.

same direction, giving rise to good radiation. Fig. 6 presents the current distributions on the feeding stub and radiating patch at two radiation null frequencies. As seen, at lower radiation null frequency ($f_{\text{Null}1}$), the energy concentrates between the patch and stub, and the induced currents have reversed directions. While for the upper radiation null case ($f_{\text{Null}2}$), the energy is attracted to the vicinity of the open slots. Similarly, the induced currents are oppositely oriented. Consequently, at these two frequencies, the radiations due to the induced currents would counteract each other, resulting in two radiation nulls.

2) PARAMETERS STUDY

Study on some key parameters has been carried out to gain deeper understanding of the working principle of the proposed filtering antenna. The performance of Design IV with different lengths of U-shaped slot and driven stub is illustrated in Fig. 7. It can be observed that as the lengths of U-shaped slot and driven stub increase, the lower resonant mode along with the radiation null will move toward the lower frequencies. Thus, one can know that the driven stub etched with a U-shaped slot plays an important role in controlling the frequency of the lower resonant mode and radiation null. The influence of the length and position of the open slot in the radiating patch is also investigated as shown in Fig. 8. We can see that the upper resonant mode and radiation null are dominated by the length of the open slot, while the position has minor effect on them. Another key parameter of the proposed antenna is the length of the radiating patch, and its effect is shown in Fig. 9. As seen, it mainly controls the middle resonant mode as well as the suppression level at stopband.

3) DESIGN GUIDELINE

According to the analysis above, a design guideline for the proposed transparent filtering antenna is recommended as follows:

- 1) Design a traditional proximity-coupled-fed patch antenna on the glass substrates.
- 2) Modify the end of feeding line as a driven stub etched with a half-wavelength U-shaped slot at the desired frequency.
- 3) Etch a pair of quarter-wavelength open slots on the radiating patch at another desired frequency.

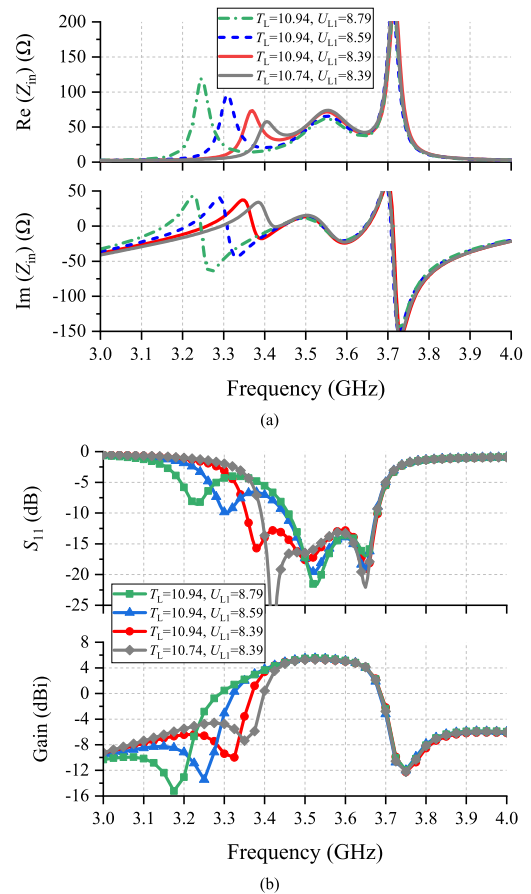


FIGURE 7. Performance of the proposed filtering antenna (Design IV) with different lengths of U-shaped slot and driven stub. (a) Input impedance. (b) Reflection coefficient and realized gain.

- 4) Add a matching stub in the feeding line and have a minor tuning of the key physical parameters to obtain excellent impedance matching and good filtering response.

III. EXPERIMENTS

A. FABRICATION PROCESS

In this work, standard photolithography and lift-off process are employed to fabricate the designed transparent filtering antenna. The fabrication process shown in Fig. 10 is described as follows: Firstly, photoresist AZ®nLOF 2070 is spin-coated onto the glass substrate and cured on a hot-plate at 110° C. Then antenna pattern window is fabricated on the photoresist by photolithography followed by standard developing process. Prior to the silver deposition, a ~10-nm Nickel layer was deposited to improve the adhesion of silver to the glass substrate. Then a ~5.5-um silver is deposited on the sample by thermal evaporation. Finally, the antenna structure is achieved by a lift-off procedure, and the two-glass substrate were aligned under a microscope and bonded by an UV-curable adhesive.

B. EXPERIMENTAL RESULTS AND DISCUSSION

The fabrication prototype of the proposed transparent filtering antenna placed on top of a piece of writing is

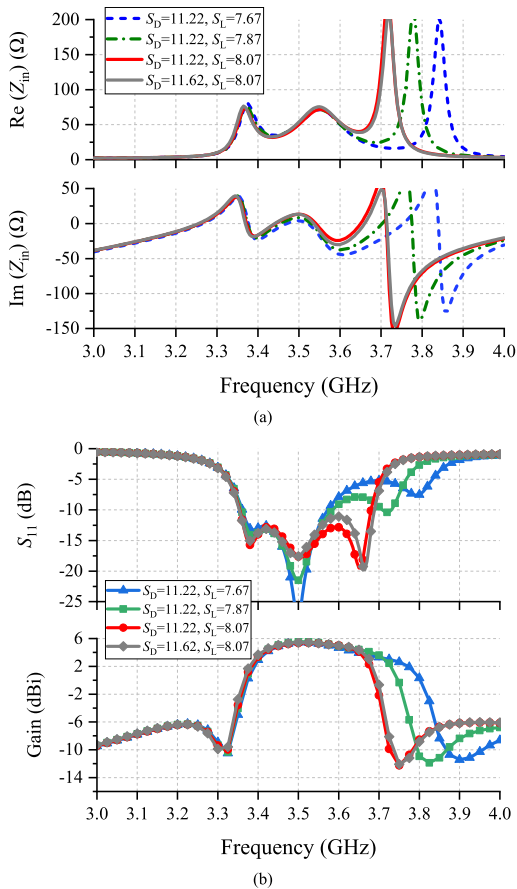


FIGURE 8. Performance of the proposed filtering antenna (Design IV) with different combination of length and position of the open slot. (a) Input impedance. (b) Reflection coefficient and realized gain.

demonstrated in Fig. 11. As shown, the writing can be read clearly. Silver paste for electric connection and adhesive for fixation were utilized to combine the antenna and SMA connector. The S-parameters were acquired by using an Agilent E8361A Network Analyzer, while the radiation performance was measured by a SATIMO system. Fig. 12 depicts the reflection coefficient as well as the gain of the proposed antenna. The measured -10 -dB impedance bandwidth is 7.6%, covering 3.41 GHz to 3.68 GHz, compared to the simulated one, 8.5% (3.36 GHz to 3.66 GHz). The measured maximum antenna gain is 4.6 dBi, while the simulated one is 5.4 dBi. In addition, the proposed antenna experiences sharp roll-off outside the operating band. A suppression level of above 10 dB is achieved at two sides of the passband. The discrepancy between the simulation and measurement is attributed to the fabrication error as well as the assembly error of minor air gap inevitably existing between the two glass substrates. The radiation patterns of the antenna are presented in Fig. 13. It exhibits low cross-polarization level in addition to good front-to-back ratio.

The antenna efficiencies of the proposed filtering antenna realized with PEC (Perfect Electric Conductor), metal mesh and CTO with sheet resistance of 1 ohm/square are shown in Fig. 14. As seen, in the simulation, only around 5%

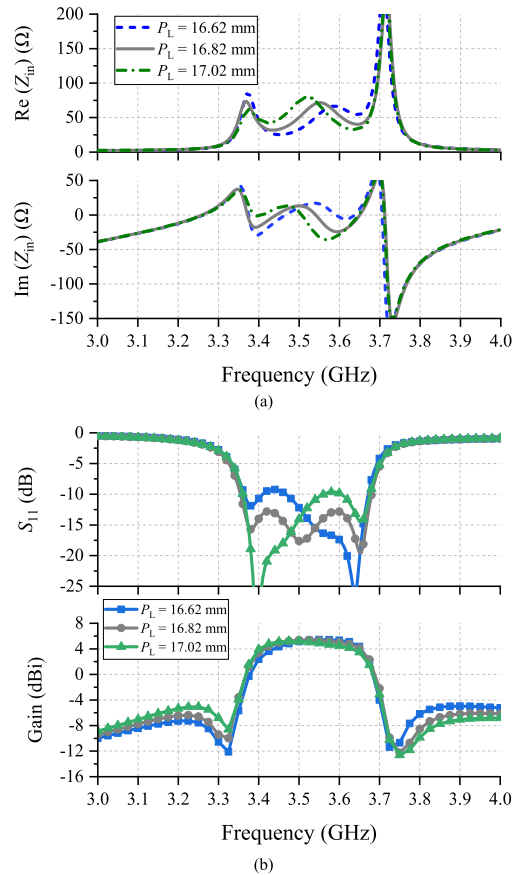


FIGURE 9. Performance of the proposed filtering antenna (Design IV) versus different length of the radiating patch. (a) Input impedance. (b) Reflection coefficient and realized gain.

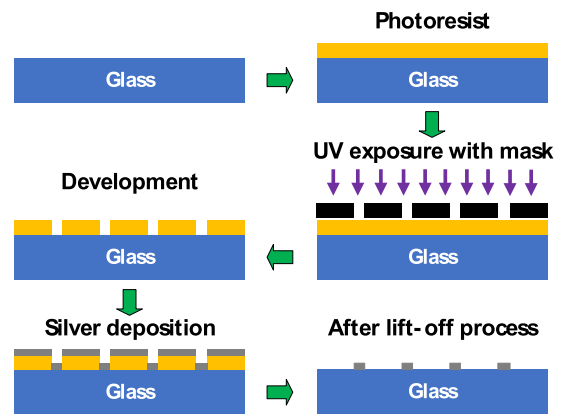


FIGURE 10. Fabrication process of the proposed transparent filtering antenna.

drop is recorded between the mesh case and PEC case. For the CTO case, the efficiency is considerably low, indicating that normal CTO suffers limited applications. The measured efficiency for the proposed transparent filtering antenna at 3.55 GHz reaches 70%.

The optical transparency of the ground region of the proposed antenna was measured with a UV 1800 from Shimadzu Schweiz GmbH. 60% of optical transparency is obtained over

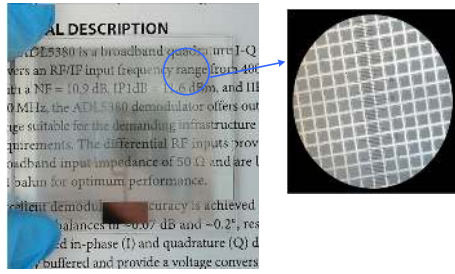


FIGURE 11. Fabricated prototype of the proposed transparent filtering antenna.

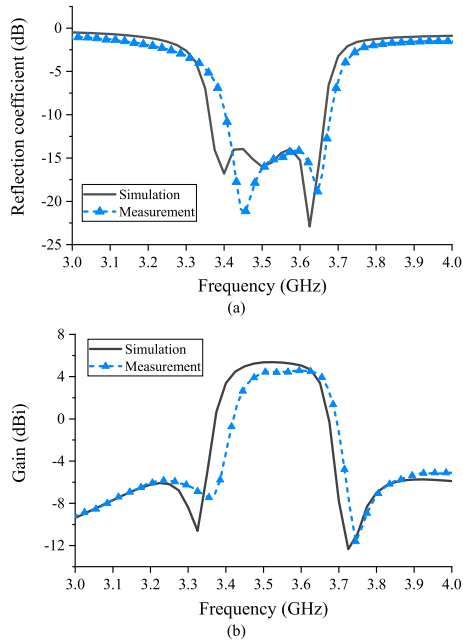


FIGURE 12. Measured and simulated performances of the proposed transparent filtering antenna. (a) Reflection coefficient. (b) Realized gain.

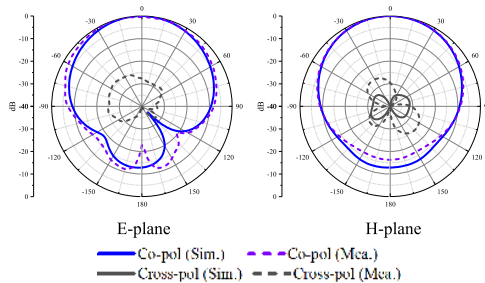


FIGURE 13. Measured and simulated radiation patterns of the proposed transparent filtering antenna at center frequency (3.55 GHz).

the entire visible light spectrum. For a single layer of such silver mesh structure, the calculated value is 73.5% [13]. Considering the additional Fresnel loss due to the glass substrate as well as the test error, the measured value makes sense. To further improve the optical transparency, one can reduce the metal density. However, that would be at the cost of getting larger loss.

A comparison among reported and proposed transparent/filtering patch antennas is illustrated in Table 2. As seen,

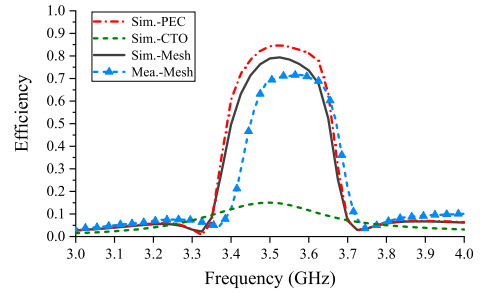


FIGURE 14. Measured and simulated antenna efficiencies of the proposed transparent filtering antenna realized with different conductive films.

TABLE 2. Comparison among reported and proposed transparent / filtering patch antenna.

Ref.	Feed Type	Filtering Response	OT	Freq. (GHz)	Imp. BW	Profile (λ_0)	FOM
[9]	Proximity coupled	No	Yes	2.45	2.66%	0.012	2.22
[10]	Direct	No	Yes	2.4	~30%	N.A.	N.A.
[11]	Direct	No	Yes	2.45	N.A.	0.01	N.A.
[12]	Direct	No	Yes	27 27.5	2.34% 11.4%	0.076 0.077	0.31 1.48
[13]	Probe	No	Yes	0.62	54.5%*	0.133	4.10*
[14]	Probe	Yes	No	2.5	19.6%	0.09	2.18
[15]	Probe	Yes	No	5.24	7%	0.03	2.33
[16]	Probe	Yes	No	3.4	23.5%	0.096	2.45
[17]	Probe	Yes	No	2.31	21.3%	0.1	2.13
[18]	Probe	Yes	No	5.44	22.6%	0.098	2.31
[19]	Probe	Yes	No	2	7%	0.03	2.33
Pro.	Proximity coupled	Yes	Yes	3.55	7.6%	0.026	2.92

λ_0 : Free space wavelength at center frequency; OT: Optically transparent;

*: -6-dB impedance matching level.

FOM = Imp. BW / Profile

compared with the reported transparent antennas, the proposed one features compact structure, enhanced bandwidth as well as good filtering response, while in comparison with the filtering antennas in the literature, it shows the advantages of low profile, no requirement of drilling as well as see-through characteristic.

IV. CONCLUSION

This paper has introduced an optically transparent proximity-coupled-fed patch antenna with enhanced impedance bandwidth and good filtering response. The antenna structure as well as its working mechanism have been fully described and investigated. Employing the standard photolithography and lift-off process, the designed antenna has been fabricated and measured. Experimental results show that the proposed antenna has an enhanced impedance bandwidth of 7.6% (3.41 GHz – 3.68 GHz) compared to the traditional one of 3.5%. The optical transparency for the ground region reaches 60%. A gain of 4.6 dBi accompanied with

above 10-dB out-of-band suppression level is achieved for the antenna. The proposed antenna features enhanced impedance bandwidth, good filtering response as well as transparent characteristic simultaneously. Without any drilling, the proposed antenna with intact ground plane is a promising candidate in applications of vehicle-to-vehicle communications and wireless indoor communications when aesthetic is also considered.

REFERENCES

- [1] F. Colombel, E. M. Cruz, M. Himdi, G. Legeay, X. Castel, and S. Vigneron, "Ultrathin metal layer, ITO film and ITO/Cu/ITO multilayer towards transparent antenna," *IET Sci., Meas. Technol.*, vol. 3, no. 3, pp. 229–234, May 2009.
- [2] T. Yasin, R. Baktur, and C. Furse, "A study on the efficiency of transparent patch antennas designed from conductive oxide films," in *Proc. IEEE Int. Symp. Antennas Propag. (APSURSI)*, Jul. 2011, pp. 3085–3087.
- [3] H. J. Song, T. Y. Hsu, D. F. Sievenpiper, H. P. Hsu, J. Schaffner, and E. Yasan, "A method for improving the efficiency of transparent film antennas," *IEEE Antennas Wireless Propag. Lett.*, vol. 7, pp. 753–756, 2008.
- [4] M. A. Malek, S. Hakimi, S. K. A. Rahim, and A. K. Evizal, "Dual-band CPW-fed transparent antenna for active RFID tags," *IEEE Antennas Wireless Propag. Lett.*, vol. 14, pp. 919–922, 2015.
- [5] S. Zarbakhsh, M. Akbari, M. Farahani, A. Ghayekhloo, T. A. Denidni, and A.-R. Sebak, "Optically transparent subarray antenna based on solar panel for CubeSat application," *IEEE Trans. Antennas Propag.*, vol. 68, no. 1, pp. 319–328, Jan. 2020.
- [6] S.-H. Park, S.-M. Lee, E.-H. Ko, T.-H. Kim, Y.-C. Nah, S.-J. Lee, J. H. Lee, and H.-K. Kim, "Roll-to-roll sputtered ITO/Cu/ITO multilayer electrode for flexible, transparent thin film heaters and electrochromic applications," *Sci. Rep.*, vol. 6, no. 1, p. 33868, Sep. 2016.
- [7] S. Hong, S. H. Kang, Y. Kim, and C. W. Jung, "Transparent and flexible antenna for wearable glasses applications," *IEEE Trans. Antennas Propag.*, vol. 64, no. 7, pp. 2797–2804, Jul. 2016.
- [8] J. R. Saberlin and C. Furse, "Challenges with optically transparent patch antennas," *IEEE Antennas Propag. Mag.*, vol. 54, no. 3, pp. 10–16, Jun. 2012.
- [9] T. Yasin and R. Baktur, "Bandwidth enhancement of meshed patch antennas through proximity coupling," *IEEE Antennas Wireless Propag. Lett.*, vol. 16, pp. 2501–2504, 2017.
- [10] W. Hong, S. Lim, S. Ko, and Y. G. Kim, "Optically invisible antenna integrated within an OLED touch display panel for IoT applications," *IEEE Trans. Antennas Propag.*, vol. 65, no. 7, pp. 3750–3755, Jul. 2017.
- [11] S. H. Kang and C. W. Jung, "Transparent patch antenna using metal mesh," *IEEE Trans. Antennas Propag.*, vol. 66, no. 4, pp. 2095–2100, Apr. 2018.
- [12] J. Park, S. Y. Lee, J. Kim, D. Park, W. Choi, and W. Hong, "An optically invisible antenna-on-display concept for millimeter-wave 5G cellular devices," *IEEE Trans. Antennas Propag.*, vol. 67, no. 5, pp. 2942–2952, May 2019.
- [13] P. D. Tung and C. W. Jung, "Optically transparent wideband dipole and patch external antennas using metal mesh for UHD TV applications," *IEEE Trans. Antennas Propag.*, vol. 68, no. 3, pp. 1907–1917, Mar. 2020.
- [14] X. Y. Zhang, W. Duan, and Y.-M. Pan, "High-gain filtering patch antenna without extra circuit," *IEEE Trans. Antennas Propag.*, vol. 63, no. 12, pp. 5883–5888, Dec. 2015.
- [15] J. Y. Jin, S. Liao, and Q. Xue, "Design of filtering-radiating patch antennas with tunable radiation nulls for high selectivity," *IEEE Trans. Antennas Propag.*, vol. 66, no. 4, pp. 2125–2130, Apr. 2018.
- [16] J.-F. Li, Z. N. Chen, D.-L. Wu, G. Zhang, and Y.-J. Wu, "Dual-beam filtering patch antennas for wireless communication application," *IEEE Trans. Antennas Propag.*, vol. 66, no. 7, pp. 3730–3734, Jul. 2018.
- [17] P. F. Hu, Y. M. Pan, X. Y. Zhang, and B.-J. Hu, "A filtering patch antenna with reconfigurable frequency and bandwidth using F-shaped probe," *IEEE Trans. Antennas Propag.*, vol. 67, no. 1, pp. 121–130, Jan. 2019.
- [18] W. Yang, Y. Zhang, W. Che, M. Xun, Q. Xue, G. Shen, and W. Feng, "A simple, compact filtering patch antenna based on mode analysis with wide out-of-band suppression," *IEEE Trans. Antennas Propag.*, vol. 67, no. 10, pp. 6244–6253, Oct. 2019.
- [19] M.-C. Tang, D. Li, Y. Wang, K.-Z. Hu, and R. W. Ziolkowski, "Compact, low-profile, linearly and circularly polarized filtennas enabled with custom-designed feed-probe structures," *IEEE Trans. Antennas Propag.*, vol. 68, no. 7, pp. 5247–5256, Jul. 2020.



HAO-TAO HU received the B.S. and M.S. degrees from the South China University of Technology, Guangzhou, Guangdong, China, in 2014 and 2017, respectively. He is currently pursuing the Ph.D. degree in electrical engineering with the City University of Hong Kong (CityU), Hong Kong.

His research interests include RF circuits and components, integration of filter and antennas, and millimetre-wave/terahertz antennas and arrays.



BAO-JIE CHEN (Member, IEEE) was born in Liaoning, China, in 1984. He received the B.S. and M.S. degrees from Dalian Polytechnic University, Dalian, China, in 2007 and 2010, respectively, both in material science, and the Ph.D. degree in electronic engineering from the City University of Hong Kong, Hong Kong, in 2014.

He is currently an Engineer with the State Key Laboratory of Terahertz and Millimeter Waves, City University of Hong Kong. His current

research interests include rare-earth-doped materials, optical amplifiers, and development of terahertz devices and components.



CHI HOU CHAN (Fellow, IEEE) received the B.S. and M.S. degrees from The Ohio State University, Columbus, OH, USA, in 1981 and 1982, respectively, and the Ph.D. degree from the University of Illinois at Urbana–Champaign, Urbana, IL, USA, in 1987, all in electrical engineering.

From 1987 to 1989, he was a Visiting Assistant Professor with the Department of Electrical and Computer Engineering, University of Illinois at Urbana–Champaign. In 1989, he joined the

Department of Electrical Engineering, University of Washington, Seattle, WA, USA, and was promoted to an Associate Professor with tenure, in 1993. In 1996, he joined the Department of Electronic Engineering, City University of Hong Kong (CityU), as a Professor, and was promoted to a Chair Professor of electronic engineering, in 1998. From 1998 to 2009, he was the first Associate Dean and then the Dean of the College of Science and Engineering, CityU. From July 2009 to September 2010, he also served as an Acting Provost for the University. He is currently the Director of the State Key Laboratory of Terahertz and Millimeter Waves, CityU. His current research interests include computational electromagnetics, millimeter-wave circuits and antennas, and terahertz science and technology. In 2002, he was elected as an IEEE Fellow with the citation of "For Contributions to Computational Electromagnetics". He received the 2019 IEEE Antennas and Propagation Society Harrington-Mitra Computational Electromagnetics Award for his fundamental contributions to fast solutions of integral equations using FFT with applications to scattering, antennas and interconnect structures in homogeneous and layered medium. He is also bestowed with the 2019 Distinguished Alumni Award from the Department of Electrical and Computer Engineering, University of Illinois at Urbana–Champaign.

...